Electromagnetically induced spatial nonlinear dispersion of four-wave mixing

Yanpeng Zhang,[1,*] Zhiqiang Nie,[1] Huaibin Zheng,[1] Changbiao Li,[1] Jianping Song,[1] and Min Xiao[2,†]
[1]*Key Laboratory for Physical Electronics and Devices of the Ministry of Education, Xi'an Jiaotong University, Xi'an 710049, China*
[2]*Department of Physics, University of Arkansas, Fayetteville, Arkansas 72701, USA*
(Received 28 February 2009; published 30 July 2009)

Spatial displacements of the probe and generated four-wave mixing beams are observed in a three-level V-type, as well as a two-level atomic system near resonance. The observed spatial shift curves reflect the typical enhanced cross-Kerr nonlinear dispersion properties in the electromagnetically induced transparency (EIT) systems. The spatial beam displacements are controlled by the strong control laser beam and the atomic density. Studying such controlled spatial beam shifts can be important in image storage and in generating spatially correlated (entangled) laser beams in multilevel EIT systems.

DOI: 10.1103/PhysRevA.80.013835 PACS number(s): 42.50.Gy, 42.65.Jx, 42.65.Tg

As two or more laser beams propagate through an atomic medium, the cross-phase modulation (XPM), as well as the modified self-phase modulation (SPM), can significantly affect the propagations and spatial patterns of the traveling laser beams. Laser beam self-focusing [1], deflection [2], beam breaking [3], and pattern formation [4,5] have been extensively studied with two laser beams propagating in (two-level) atomic vapors. It has been shown that the self- and cross-Kerr nonlinearities can be significantly enhanced and modified in three-level atomic systems due to laser-induced atomic coherence [or electromagnetically induced transparency (EIT)] [6–8]. EIT-induced waveguide effect [9], elimination of beam filamentation [10,11] by atomic coherence, and spatial all-optical switching of laser beams [12] were reported in the past few years. At the same time, four-wave mixing (FWM) processes have been significantly enhanced in three-level EIT systems [13]. Recently, strongly correlated probe and generated FWM beams [14], as well as their spatial entanglement [15], were observed in a four-level atomic system.

One of the distinct features in EIT systems is the sharp linear [16], as well as nonlinear, dispersions in frequency near the EIT resonance. In this paper, we show that by arranging laser beams in a certain spatial configuration, such sharp dispersive feature in frequency domain for the probe beam can be converted into spatial beam displacement, which exactly mimics the dispersion curve for the Kerr-nonlinear index of refraction in the EIT system [7], controlled by the strong coupling laser beam. Also, when two additional pump laser beams are applied to the probe transition, the FWM signal beam can be spatially displaced. Again, a dispersionlike spatial deflection curve for the FWM signal is seen. Such electromagnetically induced spatial dispersion (EISD) can be used for spatial switching and routing and as an easy way to measure the Kerr-nonlinear indices of refraction for the multilevel atomic media.

The three-level V-type atomic system is shown in Fig. 1(a). Three energy levels [$|0\rangle$ ($3S_{1/2}$), $|1\rangle$ ($3P_{1/2}$), and $|2\rangle$ ($3P_{3/2}$)] from sodium atoms (in a heat pipe oven without buffer gas creating a number density of approximately 10^{13} cm^{-3}) are involved in the experiments. The pulse laser beams (horizontally polarized) with diameters of about 1 mm are aligned spatially as shown in Fig. 1(c) with the control beam $\boldsymbol{E}_2$ (frequency ω_2, $\mathbf{k}_2$) and pump beams $\boldsymbol{E}_1$ (frequency ω_1, $\mathbf{k}_1$) and $\boldsymbol{E}_1'$ ($\omega_1,\mathbf{k}_1'$) propagating through the atomic medium in the same direction ($\boldsymbol{E}_1$ and $\boldsymbol{E}_2$ are collinear) with small angles ($\sim 0.3°$) between them. The probe beam $\boldsymbol{E}_p$ (ω_1, $\mathbf{k}_p$) propagates in the opposite direction with a small angle as shown in Fig. 1(c). The laser beams $\boldsymbol{E}_1$, $\boldsymbol{E}_1'$, and $\boldsymbol{E}_p$ (with Rabi frequencies G_1, G_1', and G_p, respectively, connecting the transition $|0\rangle-|1\rangle$) are from one near-transform-limited dye laser (10 Hz repetition rate, 5 ns pulse width, and 0.04 cm^{-1} linewidth). A generated one-photon resonant FWM [17] beam $\boldsymbol{E}_{F1}$ (with Rabi frequency G_{F1}) sampled by a charge coupled device (CCD) satisfies the phase-matching condition $\mathbf{k}_{F1}=\mathbf{k}_1-\mathbf{k}_1'+\mathbf{k}_p$. The control field $\boldsymbol{E}_2$ (with Rabi frequency G_2 and driving the transition $|0\rangle-|2\rangle$) is from another dye laser with the same characteristics as the first dye laser. When the beams $\boldsymbol{E}_1$, $\boldsymbol{E}_1'$, and $\boldsymbol{E}_p$ are also tuned to the same transition as $\boldsymbol{E}_2$, the system becomes an effective two-level one [Fig. 1(b)]. When the four laser beams are all on, two one-photon resonant FWM processes, $\mathbf{k}_{F1}$ and $\mathbf{k}_{F2}=\mathbf{k}_2-\mathbf{k}_1'+\mathbf{k}_p$, can be generated simultaneously. However, since $\boldsymbol{E}_{F1}$ is always the dominant one [17], we will only consider it in this work.

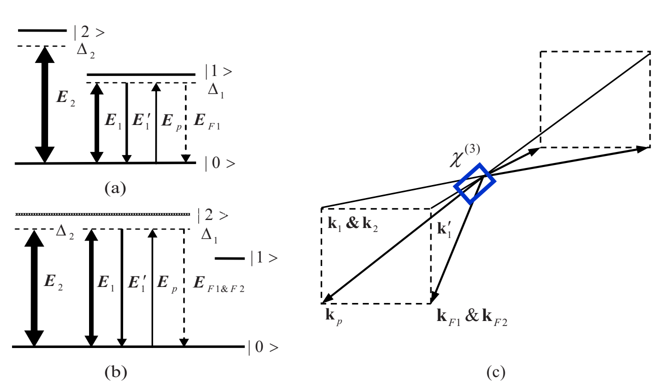

FIG. 1. (Color online) (a) Three-level V-type system with the control beam $\boldsymbol{E}_2$ ($|0\rangle-|2\rangle$) and the FWM signal $\boldsymbol{E}_{F1}$ generated by the pump beams ($\boldsymbol{E}_1,\boldsymbol{E}_1'$) and the probe beam ($\boldsymbol{E}_p$)($|0\rangle-|1\rangle$). (b) Two-level system with four laser beams tuned to the same transition. (c) Spatial beam geometry used in the experiments.

*ypzhang@mail.xjtu.edu.cn
†mxiao@uark.edu

Under our experimental conditions, the sodium vapor is an EIT-enhanced Kerr medium. The laser beam $\boldsymbol{E}_2$ (or $\boldsymbol{E}_1$) is approximately 10^2 times stronger than the beam $\boldsymbol{E}_1'$ and 10^4 times stronger than the weak beam $\boldsymbol{E}_p$, so $\boldsymbol{E}_2$ or $\boldsymbol{E}_1$ beams can control the spatial shifts of $\boldsymbol{E}_{p,F1}$. The mathematical description of the propagation properties of $\boldsymbol{E}_{p,F1}$ due to self- and cross-Kerr nonlinearities of the control and pump beams can be obtained through numerically solving the following coupled equations:

$$\frac{\partial A_p}{\partial z} - \frac{i\nabla_\perp^2 A_p}{2k_p} = \frac{ik_p}{n_0}(n_2^{S1}|A_p|^2 + 2n_2^{X1}|A_1|^2 + 2n_2^{X2}|A_2|^2)A_p, \tag{1}$$

$$\frac{\partial A_{F1}}{\partial z} - \frac{i\nabla_\perp^2 A_{F1}}{2k_{F1}} = \frac{ik_{F1}}{n_0}[n_2^{S2}|A_{F1}|^2 + 2n_2^{X3}|A_1|^2 + 2n_2^{X4}|A_2|^2 + 2n_2^{X5}|A_1'|^2]A_{F1}, \tag{2}$$

where z is the longitudinal coordinate in the propagation direction and A_1' and $A_{1,2}$ are the slowly varying envelope amplitudes of the fields $\boldsymbol{E}_1'$ and $\boldsymbol{E}_{1,2}$, respectively. $k_p=k_{F1}=\omega_1 n_0/c$ and n_0 is the linear refractive index at ω_1. $n_2^{S1,S2}$ are the self-Kerr nonlinear coefficients of $\boldsymbol{E}_{p,F1}$ and n_2^{X1-X5} are the cross-Kerr nonlinear coefficients due to the fields $\boldsymbol{E}_{1,2}$ and $\boldsymbol{E}_1'$, respectively. The Kerr nonlinear coefficients can be defined as $n_2=\mathrm{Re}\,\chi^{(3)}/(\varepsilon_0 c n_0)$, where the third-order nonlinear susceptibility is given by $\chi^{(3)}=N\mu_p^2\mu_{i0}^2\rho_{j0}^{(3)}/(\hbar^3\varepsilon_0 G_p G_i^2)$. N is atomic density. μ_p (μ_{i0}) is the dipole matrix element of the probe transition. Doppler effect and the power broadening effect are considered in calculating the Kerr nonlinear coefficients. By assuming Gaussian profiles for the input fields, Eqs. (1) and (2) are solved using the split-step method [1].

Figure 2 shows spatial displacements of beams $\boldsymbol{E}_{p,F1}$, respectively, versus frequency detuning Δ_1 ($\Delta_1=\Omega_1-\omega_1$ for the three-level system or $\Omega_2-\omega_1$ for the two-level system) with a fixed control beam ($\Delta_2=\Omega_2-\omega_2=0$). When $\boldsymbol{E}_1$ and $\boldsymbol{E}_1'$ are blocked, the measured probe beam displacement shows a spatial dispersionlike curve (triangle points). When $\boldsymbol{E}_p$ is tuned to the transition between $|0\rangle-|2\rangle$, the spatial displacements (square points) also show the similar dispersionlike curve. The data points are fitted well with the calculated cross-Kerr nonlinear coefficient n_2 vs Δ_1. The inset in Fig. 2(a) shows the images of the measured probe beam spots vs Δ_1 in the two-level system. In the region $\Delta_1<0$, the smaller beam spots indicate self-focusing effect for the probe beam due to positive self-Kerr nonlinear index, while the larger beam spots with $\Delta_1>0$ are due to self-defocusing because of the sign change in the self-Kerr nonlinear coefficient. When $\boldsymbol{E}_1$ and $\boldsymbol{E}_1'$ are on, the generated $\boldsymbol{E}_{F1}$ (in either the three-level or the two-level system) is deflected versus Δ_1, as shown in Fig. 2(b). The spatial deflection curves are well fitted with the calculated cross-Kerr nonlinear indices of refraction (solid curves) for the three-level V-type and two-level systems, respectively. The inset in Fig. 2(b) shows the images of the measured FWM beam spots versus Δ_1 in the three-level system.

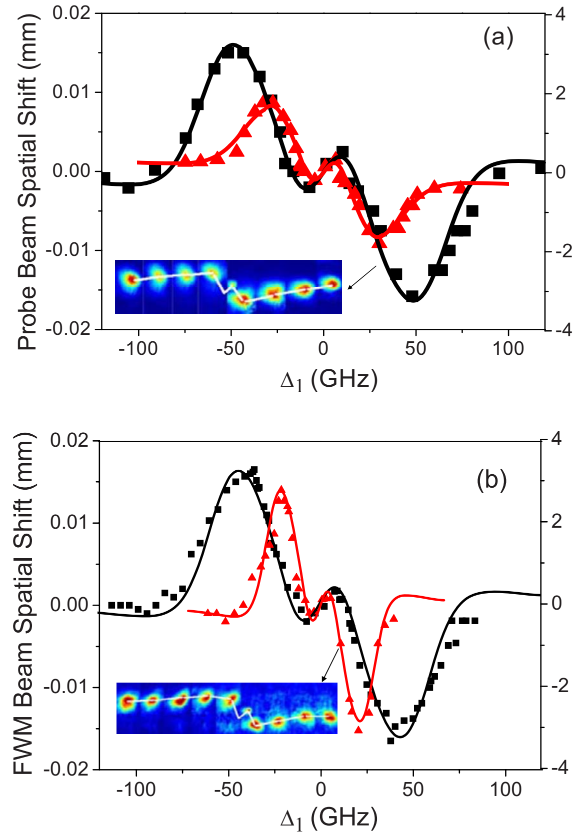

FIG. 2. (Color online) (a) EISD shifts of the beam $\boldsymbol{E}_p$ and the fitted cross-Kerr nonlinear coefficient n_2 vs Δ_1 in the two-level (squares) and three-level (triangles) systems, respectively. Inset: EISD spots of $\boldsymbol{E}_p$ versus Δ_1 in the two-level system. (b) EISD shifts of the beam $\boldsymbol{E}_{F1}$ and the fitted cross-Kerr nonlinear coefficient versus Δ_1 in the two-level (squares) and three-level (triangles) systems, respectively. Inset: EISD spots of $\boldsymbol{E}_{F1}$ vs Δ_1 in the three-level system. T=200 °C, G_p=0.2 GHz, $G_1=G_1'$=1.1 GHz, and G_2=9.7 GHz.

The observed spatial displacements of $\boldsymbol{E}_{p,F1}$ are caused by the noncollinear propagations of the laser beams and the enhanced cross-Kerr nonlinear indices of refraction by $\boldsymbol{E}_{1,2}$. For simplicity, let us only consider the strong control beam $\boldsymbol{E}_2$. During its propagation through the vapor cell, the wing of the beam $\boldsymbol{E}_2$ interacts with the intensity profile of either $\boldsymbol{E}_p$ or $\boldsymbol{E}_{F1}$ and distorts its phase profile to induce an optical waveguide through XPM. The nonlinear phase shift can be written as $\phi_{NL}=2k_{p,F1}n_2|A_2|^2 z/n_0$ and the additional transverse propagation wave vector is $\delta k_\perp=\phi_{NL}'$ [2]. In this case, when $n_2>0$, the direction of $\delta k_\perp$ is to the beam center of $\boldsymbol{E}_2$, and, therefore, $\boldsymbol{E}_{p,F1}$ is deflected closer to $\boldsymbol{E}_2$; when $n_2<0$, the direction of $\delta k_\perp$ is outward from the beam center of $\boldsymbol{E}_2$, thus $\boldsymbol{E}_{p,F1}$ is deflected away from $\boldsymbol{E}_2$. According to the expression for ϕ_{NL}, the amount of spatial shift is proportional to the cross-Kerr nonlinear coefficient, the field intensity, and the propagation distance. Hence, the spatial displacements of the probe and FWM beams result from the cross-Kerr nonlinear coefficients induced by the strong control field.

As the Rabi frequency of the control field (G_2) increases, not only the spatial displacement gets bigger but also an additional contribution, independent of the frequency detun-

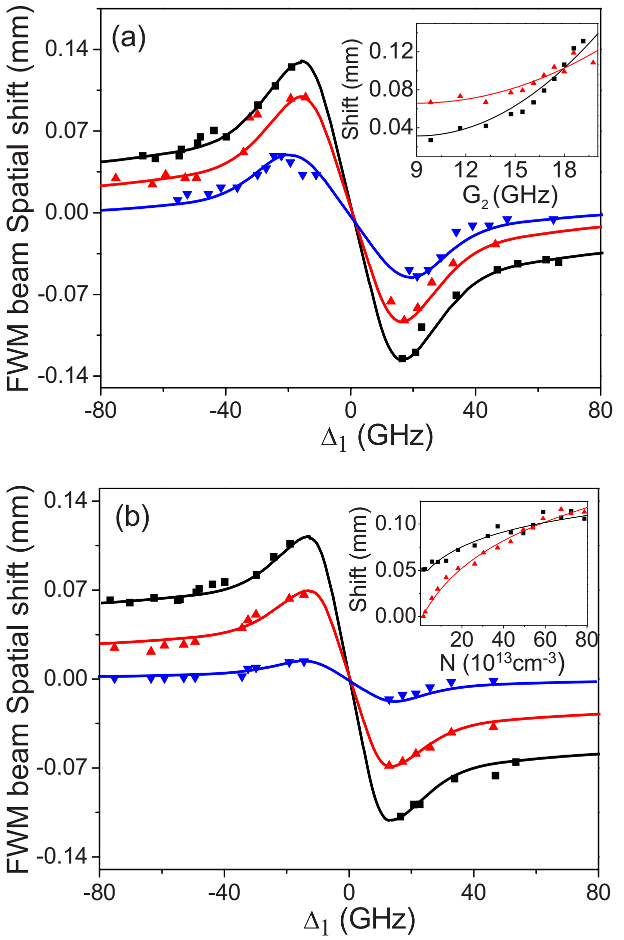

FIG. 3. (Color online) (a) Spatial dispersion curves of $\boldsymbol{E}_{F1}$ in the two-level system versus Δ_1 with $G_2=19.1$ (squares), 18.3 (triangles), and 11.7 GHz (reverse triangles) at 230 °C. Inset: the maximum spatial displacements of $\boldsymbol{E}_{F1}$ versus G_2 in two-level system (squares) and three-level V-type system (triangles). (b) Spatial dispersion curves of $\boldsymbol{E}_{F1}$ in the two-level system versus Δ_1 with $G_2=9.7$ GHz at 300 (squares), 250 (triangles), and 200 °C (reverse triangles). Inset: the maximum spatial displacements of $\boldsymbol{E}_{F1}$ versus atomic density N in the two-level system (squares) and three-level V-type system (triangles). The other parameters are $G_p=0.8$ GHz and $G_1=G_1'=3.8$ GHz. The solid lines are theoretically calculated spatial shifts.

ing Δ_1, appears, as shown in Fig. 3(a). This constant spatial displacement (the nondispersion term only depending on G_2 and N) is the dominant shift at $|\Delta_1| \gg 0$, while the dispersion displacement (n_2 dispersion term) becomes the dominant shift when Δ_1 is close to zero. Figure 3(b) presents the temperature (atomic density N) effects on the spatial displacement with a bigger spatial displacement at higher atomic density. The solid curves are the theoretically simulated spatial displacements of the FWM beam based on the coupled Eqs. (1) and (2). The differences in the maximum spatial displacements for the three-level system [Fig. 1(a)] and effective two-level system [Fig. 1(b)] as functions of G_2 and N are plotted in the insets of Figs. 3(a) and 3(b), respectively.

Let us consider the spatial displacements of the generated FWM beams with all the control and pump beams on but

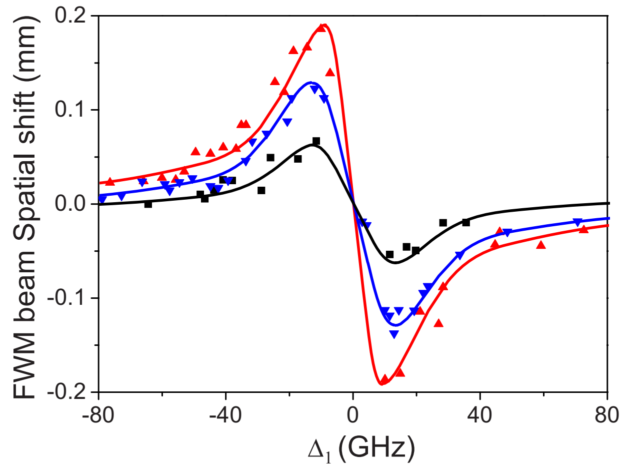

FIG. 4. (Color online) Spatial dispersion curves of $\boldsymbol{E}_{F1}$ in the two-level system versus Δ_1 dressed by $\boldsymbol{E}_2$ (squares), $\boldsymbol{E}_1$ (triangles), and both $\boldsymbol{E}_2$ and $\boldsymbol{E}_1$ (reverse triangles) at 240 °C. The solid lines are the theoretically calculated spatial displacements. $G_1=G_2=17.6$ GHz and $G_1'=3.8$ GHz, $G_p=0.8$ GHz.

with different relative intensities. Other than the case of having a strong control beam as discussed above (i.e., $G_2 \gg G_1, G_1' \gg G_p > G_{F1}$), we can also let $\boldsymbol{E}_1$ to be quite strong (i.e., $G_1 \gg G_2, G_1' \gg G_p > G_{F1}$), which is the singly-dressing scheme, or let both $\boldsymbol{E}_{1,2}$ to be strong (i.e., $G_1, G_2 \gg G_1' \gg G_p > G_{F1}$), which is the doubly-dressing scheme [18]. Under these different conditions, the strong laser fields dress the energy levels differently and modify the degree of spatial deflections for the FWM beam (Fig. 4).

Now, let us consider the two-level system as an example. First, when $\boldsymbol{E}_2$ is the only strong field, it dresses the level $|0\rangle$ to create the dressed states $|G_2\pm\rangle$. Second, let $\boldsymbol{E}_1$ be the only strong field. Since $\boldsymbol{E}_1$ and $\boldsymbol{E}_p$ have the same frequency detuning Δ_1, the upper-level $|2\rangle$ and the lower-level $|0\rangle$ are always on resonance with and dressed by $\boldsymbol{E}_1$. In this case, two pairs of dressed states $|G_1\pm\rangle$ generate. For $\boldsymbol{E}_1$ is resonant dressing and $\boldsymbol{E}_2$ nonresonant dressing [17], the strong $\boldsymbol{E}_1$ field induces a larger XPM than the strong $\boldsymbol{E}_2$ field can do, so the spatial displacement of $\boldsymbol{E}_{F1}$, controlled by the stronger $\boldsymbol{E}_1$ field, is larger than that by the stronger $\boldsymbol{E}_2$ field. Third, when both $\boldsymbol{E}_1$ and $\boldsymbol{E}_2$ fields are strong ones (doubly-dressing case) since they share the common level $|0\rangle$ and interact with each other [18]. The destructive interaction results that the XPM induced by the doubly-dressing fields is weaker than the sum of the effects due to singly dressing by $\boldsymbol{E}_1$ and $\boldsymbol{E}_2$ alone in Fig. 4.

The spatial displacements of the probe and FWM beams are mainly determined and controlled by the large cross-Kerr nonlinear coefficients of the strong laser fields. However, the cross-Kerr effects induced by the relatively weaker pump beam(s) can also exist as a secondary effect to the spatial displacements. When $\boldsymbol{E}_{p,F1}$ get stronger (with a strong probe and a more efficient FWM process), coupled soliton pairs can form with $\boldsymbol{E}_{p,F1}$ beams. Bright-bright soliton pair in the self-focusing region and the dark-dark soliton pair in the self-defocusing region can form and propagate in such EIT media [4]. The enhanced self-Kerr and cross-Kerr nonlinear coefficients due to induced atomic coherence (or EISD) enable the formations of such spatial soliton pairs with much lower input laser powers, which can be very important for their applications in optical communications. Moreover, the current work opens the doors for further studies on formations of spatially correlated (entangled) laser beams [15] and storage of images [19] in multilevel coherent atomic systems.

This work was supported by NSFC (Grant No. 60678005), FANEDD (Grant No. 200339), RFDP (Grant No. 20050698017), FYTEFYTIHEC (Grant No. 101061), and NCET (Grant No. 08-0431).

[1] G. P. Agrawal, Phys. Rev. Lett. **64**, 2487 (1990).
[2] A. J. Stentz *et al.*, Opt. Lett. **17**, 19 (1992).
[3] J. M. Hickmann, A. S. L. Gomes, and C. B. de Araujo, Phys. Rev. Lett. **68**, 3547 (1992).
[4] A. S. Desyatnikov, A. A. Sukhorukov, and Y. S. Kivshar, Phys. Rev. Lett. **95**, 203904 (2005).
[5] R. S. Bennink, V. Wong, A. M. Marino, D. L. Aronstein, R. W. Boyd, C. R. Stroud, S. Lukishova, and D. J. Gauthier, Phys. Rev. Lett. **88**, 113901 (2002).
[6] S. E. Harris, Phys. Today **50**(7), 36 (1997).
[7] H. Wang, D. Goorskey, and M. Xiao, Phys. Rev. Lett. **87**, 073601 (2001).
[8] S. E. Harris and Y. Yamamoto, Phys. Rev. Lett. **81**, 3611 (1998).
[9] A. G. Truscott, M. E. J. Friese, N. R. Heckenberg, and H. Rubinsztein-Dunlop, Phys. Rev. Lett. **82**, 1438 (1999).
[10] M. Jain *et al.*, Phys. Rev. Lett. **77**, 4326 (1996).
[11] O. Firstenberg, M. Shuker, N. Davidson, and A. Ron, Phys. Rev. Lett. **102**, 043601 (2009).
[12] A. M. C. Dawes *et al.*, Science **308**, 672 (2005).
[13] Y. Li and M. Xiao, Opt. Lett. **21**, 1064 (1996).
[14] V. Boyer, A. M. Marino, and P. D. Lett, Phys. Rev. Lett. **100**, 143601 (2008).
[15] V. Boyer *et al.*, Science **321**, 544 (2008).
[16] M. Xiao, Y. Q. Li, S. Z. Jin, and J. Gea-Banacloche, Phys. Rev. Lett. **74**, 666 (1995).
[17] H. B. Zheng *et al.*, Appl. Phys. Lett. **93**, 241101 (2008).
[18] Z. Nie, H. Zheng, P. Li, Y. Yang, Y. Zhang, and M. Xiao, Phys. Rev. A **77**, 063829 (2008).
[19] M. Shuker, O. Firstenberg, R. Pugatch, A. Ron, and N. Davidson, Phys. Rev. Lett. **100**, 223601 (2008).